

# A Compact Design of a Two-stage Piecewise Linear ADC Used for Sensor Linearity Improvement

Jelena Jovanovic\* , Dragan Denić

*Department of Measurements, University of Niš, Faculty of Electronic Engineering, Aleksandra Medvedeva, 4, 18000, Niš, Serbia, [jelena.jovanovic@elfak.ni.ac.rs](mailto:jelena.jovanovic@elfak.ni.ac.rs), [dragan.denic@elfak.ni.ac.rs](mailto:dragan.denic@elfak.ni.ac.rs)*

**Abstract:** This paper presents a compact two-stage piecewise linear analog-to-digital converter (ADC) that enhances sensor linearity while featuring a reduced design complexity. Unlike a traditional two-stage piecewise linear ADC, the proposed architecture achieves the same resolution with fewer components by using a single flash ADC for both conversion stages and by adding a comparator at the start of each conversion stage. The flash ADC has a resolution of  $(n/2-1)$  bits, where  $n$  is the total resolution of the two-stage piecewise linear ADC. This compact architecture enables efficient and simultaneous linearization and digitization of sensor output while significantly reducing energy consumption and implementation costs. Numerical results confirm the compactness and cost-effectiveness of the proposed design, showing up to a 75 % reduction in comparator count and up to a 25 % reduction in resistor count compared to the traditional design of the two-stage piecewise linear ADC with the same total resolution. These significant savings make the proposed two-stage piecewise linear ADC design well-suited for applications with strict energy and space constraints.

**Keywords:** sensor linearization, flash ADC, two-stage piecewise linear ADC, comparator count, resistor count, compact design

## 1. INTRODUCTION

Accurate sensor measurements are essential in modern measurement systems, yet sensor nonlinearity remains a significant challenge affecting overall accuracy. Several techniques can address this issue, but the use of a two-stage piecewise linear analog-to-digital converter (ADC) has proven highly effective for sensor linearization [1]-[10]. By integrating sensor linearization and signal digitization into a single process, the mentioned ADC reduces processing time, power consumption and implementation costs, making it highly suitable for resource-constrained measurement applications. Because of these advantages, two-stage piecewise linear ADCs are widely used for the linearization of various sensor types, including NTC thermistors, Pt100 sensors, angular position sensors, and humidity sensors [1]-[7], [11].

Other sensor linearization techniques often suffer from limitations such as high memory and computational demands, particularly when the sensor's transfer function is unknown [12], [13]. Although neural networks have been explored as an alternative approach, their implementation requires large amounts of training data and significant computational resources [12], [14], [15]. In contrast, the two-stage piecewise linear ADC performs sensor linearization without these overheads, providing a more resource-efficient solution.

The traditional two-stage piecewise linear ADC architecture uses a separate ADC for each conversion stage. Linearization is performed in the first stage with a flash ADC whose transfer function approximates, in a piecewise linear manner, the inverse of the sensor's static transfer function. The input range of the flash ADC is divided into segments of varying widths (nonuniform segments), each bounded by specific points called break voltages. These break voltages are used as reference voltages for the comparators in the flash ADC. In the second conversion stage, a linear ADC is used, which may be implemented as a flash ADC or as another type, such as a successive approximation (SAR) ADC. Within the second conversion stage, each input voltage sample is further mapped to a uniform sub-segment within the corresponding nonuniform segment defined earlier. Although linearization is not performed in this stage, the subdivision improves both resolution and measurement accuracy. The resolutions of the first and second conversion stages are usually not equal. It is generally preferable for the first stage to have higher resolution, as sensor linearization primarily occurs at this stage. However, increasing the resolution of the first stage also increases implementation complexity.

An advantage of a two-stage piecewise linear ADC is its adaptability to different sensor types by adjusting the comparators' reference voltages in the flash ADC using a resistor ladder network. Given this advantage, reducing the

complexity, power consumption, and implementation costs of the two-stage piecewise linear ADC remains an important research objective.

This paper presents a compact and cost-effective design for a two-stage piecewise linear ADC, in which both conversion stages are performed using a single flash ADC, with the addition of two comparators, one at the start of each conversion stage. This design strategy significantly reduces the overall comparator and resistor counts. Notably, in the proposed design, each additional comparator contributes one bit of resolution, unlike the traditional approach, where increasing the resolution of a conversion stage by one bit doubles the number of comparators.

## 2. SUBJECT & METHODS

This paper proposes a compact two-stage piecewise linear ADC designed to improve sensor linearity and increase measurement accuracy. The key contribution of the proposed design is a substantial reduction in component count compared to traditional architecture. Unlike traditional two-stage piecewise linear ADC implementation (see Fig. 1), the proposed approach achieves the same total resolution with significantly fewer comparators by reusing a single flash ADC for both conversion stages and incorporating only two additional comparators. Although several methods for increasing resolution with fewer comparators have been explored in the literature [5], [6], [16], the proposed design achieves greater compactness by further reducing the number of resistors required in the flash ADC's resistor ladder network [17], [18]. Since comparators are among the most power-consuming components in flash ADC circuits [19], reducing their number, as well as the number of resistors, decreases circuit complexity, power consumption and implementation costs. This makes the proposed design a highly efficient alternative to the traditional two-stage piecewise linear ADC design.

Fig. 1 illustrates a traditional 6-bit two-stage piecewise linear ADC, where each conversion stage uses a separate flash ADC. It is well established that the implementation of an  $N$ -bit flash ADC requires  $2^N$  resistors and  $2^N-1$  comparators [17], [18]. In the example shown in Fig. 1, two 3-bit flash ADCs are used, resulting in a total of 14 comparators (7 per stage) and 16 resistors across two independent resistor ladder networks. The input range of the first conversion stage spans from 0 V to  $V_{MAX}$  ( $V_{MAX} = f(x_{MAX})$ ), where  $f(x)$  is the sensor's transfer function and  $x_{MAX}$  is the maximum value of the measured parameter  $x$ , and the current sample of the input voltage signal is denoted as  $V_{IN}$ . In this example, both stages are configured with the same resolution; however, this configuration is not a requirement in practical implementations. Typically, the first stage is implemented with a lower resolution than the second due to the complexity of designing a nonuniform resistor ladder network ( $R_1$  to  $R_8$ ), which determines the reference voltages for the comparators. However, higher resolution in the first stage is desirable, as linearization is performed at that point.

The second stage is simpler to implement, using a uniform resistor ladder network composed of identical resistors  $R$ . This allows the use of uniform off-the-shelf ADCs in the

second stage (e.g., flash, SAR, or other types) [1]-[4], [6], [11], [20]. Equal resolutions of 3 bits per conversion stage were chosen in the traditional architecture, shown in Fig. 1, to enable a direct comparison with the compact 6-bit two-stage piecewise linear ADC proposed in this paper.

The proposed 6-bit architecture, shown in Fig. 2, differs fundamentally by replacing two 3-bit flash ADCs with a single 2-bit flash ADC and two additional comparators. Each of these comparators ( $C_1$  and  $C_5$ ) independently contributes one bit of resolution. Determining the nonuniform reference voltages of all comparators  $V_i$  in the first conversion stage, including the reference voltage  $V_{REF1}$  of the additional comparator  $C_1$  (see Fig. 2), is a critical aspect of the design. These voltages can be determined using the following equations:

$$V_i = f(x_i), \quad i = 1, 2, \dots, 2^{n/2} - 1, \quad (1)$$

$$V_{REF1} = f(x_i), \quad i = 2^{n/2-1}, \quad (2)$$

for the corresponding values  $x_i$  at the sensor input, defined as:

$$x_i = i \cdot \frac{x_{MAX}}{2^{n/2}}, \quad i = 1, 2, \dots, 2^{n/2} - 1. \quad (3)$$

The resistor values used to set these reference voltages are determined as follows:

$$R_i = \frac{R_t}{V_{MAX}} \cdot V_i - \sum_{j=1}^{i-1} R_j, \quad i = 1, 2, \dots, 2^{n/2}, \quad (4)$$

where  $R_t$  represents the total resistance of the resistor ladder network used in the first conversion stage.

In the proposed two-stage piecewise linear ADC (see Fig. 2), the initial step is to set the reference voltage  $V_{REF1}$  of comparator  $C_1$ , which corresponds to the central reference voltage  $V_4$ . The input sample  $V_{IN}$  is captured at a moment determined by the timing generator signal  $t_1$ . The sample is then routed to the input of comparator  $C_1$ . Comparator  $C_1$  evaluates whether the input sample  $V_{IN}$  is greater than or less than the voltage  $V_{REF1}$ . If  $V_{IN} > V_{REF1}$ , the output bit  $B'_2 = 1$ ; otherwise,  $B'_2 = 0$ . This bit controls three 2-to-1 analog multiplexers, which route either the reference voltages less than  $V_{REF1}$  or those greater than  $V_{REF1}$  to the inputs of the flash ADC comparators, depending on the value of  $V_{IN}$ . As a result, the input range of the flash ADC is dynamically selected as either from 0 to  $V_{REF1}$  when  $B'_2 = 0$ , or from  $V_{REF1}$  to  $V_{MAX}$  when  $B'_2 = 1$ . After selecting the relevant reference voltages and comparing them against  $V_{IN}$ , a 3-bit code is generated and then converted into a 2-bit binary code by a priority encoder, producing the output bits  $B'_1$  and  $B'_0$ . The combined bits  $B'_2B'_1B'_0$  represent the result of the coarse stage and are stored in the output register at the timing signal  $t_2$ . These bits also control two 8-to-1 analog multiplexers, which select the corresponding lower  $V_L$  and upper  $V_U$  reference (break) voltages representing the boundaries of the nonuniform segment to which the input sample  $V_{IN}$  belongs. Simultaneously,  $V_L$  and  $V_U$  define the input range for the second stage of conversion.



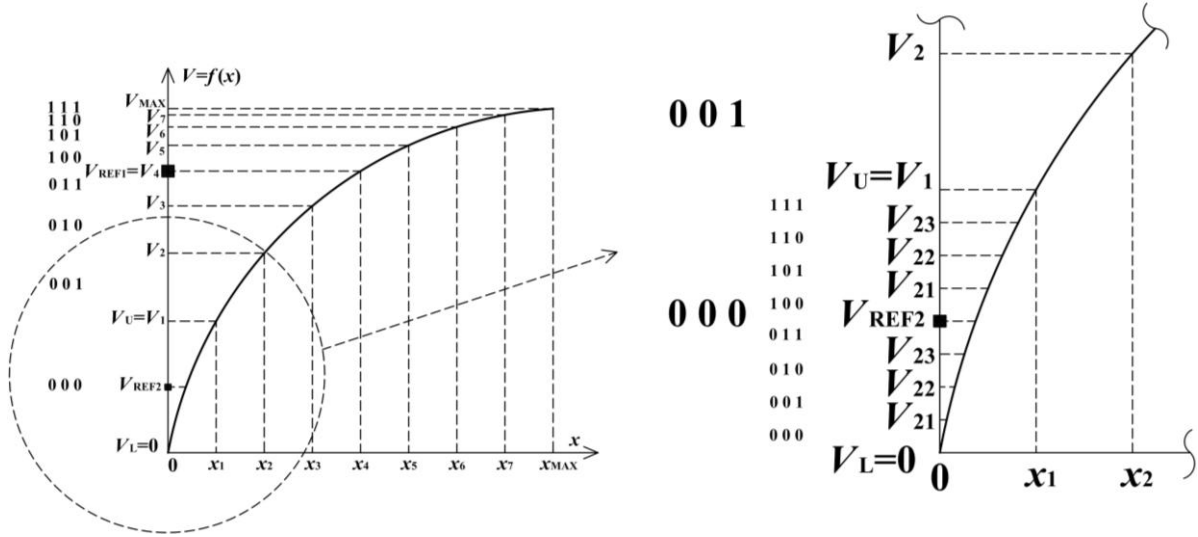


Fig. 3. Illustration of a method for determining the break voltages of nonuniform segments ( $V_1$  to  $V_7$ ) in the first conversion stage and the break voltages of uniform sub-segments ( $V_{21}$ ,  $V_{22}$ , and  $V_{23}$ ) in the second conversion stage (enlarged detail on the right).

Fig. 3 illustrates the method for determining the break voltages of the nonuniform segments ( $V_1$  to  $V_7$ ) in the first conversion stage and the break voltages of the uniform sub-segments ( $V_{21}$ ,  $V_{22}$ , and  $V_{23}$ ) in the second conversion stage. By dividing the sensor's input range, which spans from 0 to  $x_{MAX}$ , into eight equal parts (for  $n = 3$  bits) and mapping the boundaries of these divisions onto the corresponding values on the y-axis, the break voltages of the eight nonuniform segments are obtained. Each nonuniform segment is encoded with a corresponding 3-bit binary code ranging from 000 to 111. Depending on the input voltage sample  $V_{IN}$ , one of these nonuniform segments serves as the input range for the second, uniform conversion stage (between  $V_L$  and  $V_U$ ). The right side of Fig. 3 presents a detailed view explaining how the uniform break voltages  $V_{21}$ ,  $V_{22}$ , and  $V_{23}$  are determined in the second conversion stage (for example, when  $V_L = 0$  V and  $V_U = V_1$ ). In this case, the reference voltage  $V_{REF2}$  also influences the values of the break voltages for the uniform sub-segments, as it defines the input range for the flash ADC in the second stage. Each of these uniform sub-segments is also represented by a unique 3-bit code word, ranging from 000 to 111. The values of the break (reference) voltages  $V_{2j}$  in the second conversion stage can be determined as follows:

$$1) V_{IN} < V_{REF2}, \quad (B''_2 = 0), \quad (6)$$

$$V_{2j} = V_L + j \cdot \frac{V_{REF2} - V_L}{2^{n/2-1}}, \quad j = 1, 2, \dots, 2^{n/2-1} - 1, \quad (7)$$

or

$$2) V_{IN} > V_{REF2}, \quad (B''_2 = 1), \quad (8)$$

$$V_{2j} = V_{REF2} + j \cdot \frac{V_U - V_{REF2}}{2^{n/2-1}}, \quad j = 1, 2, \dots, 2^{n/2-1} - 1. \quad (9)$$

Once the switches are closed under the control of timing signal  $t_3$ , the new reference voltages  $V_{23}$ ,  $V_{22}$ , and  $V_{21}$  are applied to the inputs of comparators  $C_2$ ,  $C_3$ , and  $C_4$ , respectively. This is followed by the conversion of a 3-bit code into a 2-bit binary code using a 2-bit priority encoder, which produces the final two bits of the digital output,  $B''_1$  and  $B''_0$ . When the full 3-bit code  $B''_2B''_1B''_0$  is latched into

the output register at the moment defined by timing signal  $t_4$ , the conversion process is complete, resulting in a digital representation of the input voltage sample  $V_{IN}$ .

It is important to emphasize that after converting the complete 6-bit code  $B''_2B''_1B''_0B''_2B''_1B''_0$  back to an analog voltage, and consequently to the corresponding value of the measured parameter, a significantly smaller discrepancy can be expected between the actual and measured values [1]-[7]. In other words, the measurement error caused by the sensor's nonlinearity can be considerably reduced with the proposed linearization circuit.

### 3. RESULTS

This section provides a comparative analysis of how the resolution of a two-stage piecewise linear ADC affects the comparator and resistor requirements in both traditional and proposed compact designs. For the traditional two-stage piecewise linear ADC, the total number of comparators  $n_{ct}$  and resistors  $n_{rt}$  can be determined using the following expressions [17], [18]:

$$n_{ct} = (2^{N_t} - 1) + (2^{N_t} - 1), \quad (10)$$

$$n_{rt} = 2^{N_t} + 2^{N_t}. \quad (11)$$

Here,  $N_t = n/2$  represents the resolution of each flash ADC in the traditional two-stage configuration, where  $n$  denotes the total resolution. Each addend in both expressions corresponds to one conversion stage.

In the proposed compact two-stage piecewise linear ADC design, the total number of employed comparators  $n_{cp}$  is:

$$n_{cp} = 1 + (2^{N_p} - 1) + 1. \quad (12)$$

In this expression, the two addends with a value of 1 represent the additional comparators  $C_1$  and  $C_5$ , while the addend  $(2^{N_p}-1)$  corresponds to the number of comparators used in the flash ADC with a resolution of  $N_p = n/2-1$ . The total number of resistors used in the proposed compact design  $n_{rp}$  is given by:

$$n_{rp} = 2^{N_p+1} + (2 + 2^{N_p}), \quad (13)$$

where the first addend represents the resistors used in the resistor ladder network of the flash ADC during the first conversion stage. The second addend accounts for the two resistors forming the passive voltage divider, along with the resistors in the resistor ladder network used in the second conversion stage.

To assess the improvements introduced by the compact design compared to the traditional approach, the relative differences in comparator counts  $\delta_c$  and resistor counts  $\delta_r$  are computed as follows:

$$\delta_c = \frac{(n_{ct} - n_{cp})}{n_{ct}} \cdot 100 \%, \quad (14)$$

$$\delta_r = \frac{(n_{rt} - n_{rp})}{n_{rt}} \cdot 100 \%. \quad (15)$$

Table 1 presents key parameters for various total resolution values  $n$ , including flash ADC resolutions,  $N_t = n/2$  for the traditional design and  $N_p = n/2 - 1$  for the proposed design. It also lists comparator and resistor counts for both architectures, along with their relative differences, highlighting the hardware savings of the proposed architecture.

Table 1. Numerical values of key parameters for various total resolution values  $n$ .

| $n$ | $N_t$ | $N_p$ | $n_{ct}$ | $n_{rt}$ | $n_{cp}$ | $n_{rp}$ | $\delta_c$ [%] | $\delta_r$ [%] |
|-----|-------|-------|----------|----------|----------|----------|----------------|----------------|
| 6   | 3     | 2     | 14       | 16       | 5        | 14       | 64.2857        | 12.5000        |
| 8   | 4     | 3     | 30       | 32       | 9        | 26       | 70.0000        | 18.7500        |
| 10  | 5     | 4     | 62       | 64       | 17       | 50       | 72.5806        | 21.8750        |
| 12  | 6     | 5     | 126      | 128      | 33       | 98       | 73.8095        | 23.4375        |
| 14  | 7     | 6     | 254      | 256      | 65       | 194      | 74.4094        | 24.2187        |
| 16  | 8     | 7     | 510      | 512      | 129      | 386      | 74.7059        | 24.6094        |
| 18  | 9     | 8     | 1022     | 1024     | 257      | 770      | 74.8532        | 24.8047        |
| 20  | 10    | 9     | 2046     | 2048     | 513      | 1538     | 74.9267        | 24.9023        |
| 22  | 11    | 10    | 4094     | 4096     | 1025     | 3074     | 74.9634        | 24.9512        |
| 24  | 12    | 11    | 8190     | 8192     | 2049     | 6146     | 74.9817        | 24.9756        |
| 26  | 13    | 12    | 16382    | 16384    | 4097     | 12290    | 74.9908        | 24.9878        |
| 28  | 14    | 13    | 32766    | 32768    | 8193     | 24578    | 74.9954        | 24.9939        |
| 30  | 15    | 14    | 65534    | 65536    | 16385    | 49154    | 74.9977        | 24.9969        |
| 32  | 16    | 15    | 131070   | 131072   | 32769    | 98306    | 74.9989        | 24.9985        |

#### 4. DISCUSSION

As the total resolution  $n$  increases, the difference in the number of comparators and resistors between the traditional and proposed two-stage piecewise linear ADC designs becomes more pronounced. As previously noted, Table 1 lists the total number of comparators  $n_{ct}$  and resistors  $n_{rt}$  for the traditional design, along with the corresponding values for the proposed compact design  $n_{cp}$  and  $n_{rp}$  across various resolution values  $n$ . It also includes the calculated relative differences in comparator counts  $\delta_c$  and resistor counts  $\delta_r$  between the two designs.

The numerical results clearly demonstrate a significant reduction in hardware complexity achieved by the proposed design. As the total resolution  $n$  increases, the relative differences  $\delta_c$  and  $\delta_r$  grow steadily. Specifically, for resolutions exceeding 14 bits, both metrics show a strong upward trend, approaching their maximum values of 75 % and 25 %, respectively. These peak values will be fully attained when the total resolution reaches 42 bits. Even at lower resolutions  $n$ , the savings in component count are considerable, highlighting the cost-effectiveness of the proposed solution. This reduction translates directly into lower manufacturing costs, improved compactness, and

reduced power consumption, making the proposed two-stage piecewise linear ADC highly suitable for sensor linearization in embedded or resource-constrained systems.

It should be noted that the introduction of comparators  $C_1$  and  $C_5$ , together with additional multiplexers, causes a certain increase in conversion time. However, this is compensated by performing linearization and analog-to-digital conversion within a single circuit, which reduces the overall time required to process the sensor output signal, as well as the associated implementation cost.

#### 5. CONCLUSION

This paper presents a novel compact two-stage piecewise linear ADC that improves sensor linearity while exhibiting reduced hardware complexity. By sharing a single flash ADC between both conversion stages and introducing two additional comparators, one for each stage, the proposed design achieves the same total resolution as the traditional design but with a substantially lower component count. Analytical expressions and numerical analysis show that the proposed architecture requires significantly fewer comparators and resistors than its traditional counterpart, with the savings becoming more pronounced as total resolution increases.

The numerical results validate the advantages of the proposed compact design. At higher total resolutions, the compact design achieves up to a 75 % reduction in comparator count and up to a 25 % reduction in resistor count compared to the traditional two-stage piecewise linear ADC with the same total resolution. These reductions directly lead to lower energy consumption, reduced silicon area, and decreased manufacturing costs. Even at low and moderate resolutions, the proposed design yields notable savings, confirming its suitability for compact, low-power embedded applications. Furthermore, by combining sensor linearization with digital conversion in a single process, the two-stage piecewise linear ADC delivers improved performance in modern smart sensing systems. Overall, the results confirm that the proposed compact two-stage piecewise linear ADC is a highly efficient, scalable, and cost-effective solution for high-resolution, low-power sensor linearization.

#### ACKNOWLEDGMENT

This work was supported by the Ministry of Science, Technological Development and Innovation of the Republic of Serbia [Grant Number: 451-03-137/2025-03/200102].

#### REFERENCES

- [1] Jovanović, J., Denić, D. (2025). A double-nonuniform single-flash piecewise linear ADC used for linearization of sinusoidal sensors. *Journal of Electrical Engineering*, 76 (3), 200-210. <https://doi.org/10.2478/jee-2025-0021>
- [2] Živanović, D., Lukić, J., Denić, D. (2014). A novel linearization method of sin/cos sensor signals used for angular position determination. *Journal of Electrical Engineering and Technology*, 9 (4), 1437-1445. <https://doi.org/10.5370/JEET.2014.9.4.1437>
- [3] Lukić, J., Denić, D. (2015). A novel design of an NTC thermistor linearization circuit. *Metrology and Measurement Systems*, 22 (3), 351-362. <https://doi.org/10.1515/mms-2015-0035>
- [4] Jovanović, J., Denić, D. (2021). Mixed-mode method used for Pt100 static transfer function linearization. *Measurement Science Review*, 21 (5), 142-149. <https://doi.org/10.2478/msr-2021-0020>
- [5] Jovanović, J., Denić, D. (2021). NTC thermistor nonlinearity compensation using Wheatstone bridge and novel dual-stage single-flash piecewise-linear ADC. *Metrology and Measurement Systems*, 28 (3), 523-537. <https://doi.org/10.24425/mms.2021.136616>
- [6] Lopez-Martin, A. J., Zuza, M., Carlosena, A. (2003). A CMOS A/D converter with piecewise linear characteristic and its application to sensor linearization. *Analog Integrated Circuits and Signal Processing*, 36 (1), 39-46. <https://doi.org/10.1023/A:1024437311497>
- [7] Jovanović, J., Denić, D., Jovanović, U., Živanović, D. (2021). Nonlinearity compensation and accuracy improvement method for an optical rotary encoder. *Facta Universitatis, Series: Automatic Control and Robotics*, 20 (3), 167-178. <https://doi.org/10.22190/FUACR211101013J>
- [8] Sengupta, S., Johnston, M. L. (2019). Two-step, piecewise-linear SAR ADC with programmable transfer function. *Electronics Letters*, 55 (8), 444-446. <https://doi.org/10.1049/el.2019.0138>
- [9] Santos, M., Horta, N., Guilherme, J. (2014). A survey on nonlinear analog-to-digital converters. *Integration*, 47 (1), 12-22. <https://doi.org/10.1016/j.vlsi.2013.06.001>
- [10] Ananthi, S., Chaudhary, H., Singh, K. (2019). Design of read circuitry for nonlinear smart sensors. In *IOP Conference Series: Materials Science and Engineering*. IOP Publishing Ltd, 594 (1), 012036. <https://dx.doi.org/10.1088/1757-899X/594/1/012036>
- [11] Jovanović, J., Denić, D., Jovanović, U. (2017). An improved linearization circuit used for optical rotary encoders. *Measurement Science Review*, 17 (5), 241-249. <https://doi.org/10.1515/msr-2017-0029>
- [12] Islam, T., Mukhopadhyay, S. C. (2019). Linearization of the sensors characteristics: A review. *International Journal on Smart Sensing and Intelligent Systems*, 12 (1), 1-21. <https://doi.org/10.21307/ijssis-2019-007>
- [13] Šturcel, J., Kamenský, M. (2006). Function approximation and digital linearization in sensor systems. *ATP Journal PLUS*, 2, 13-17.
- [14] Ghosh, R., Nag, S., Gupta, R. (2021). A software-based linearization technique for thermocouples using recurrent neural network. In *2021 IEEE Mysore Sub Section International Conference (MysuruCon)*. IEEE, 302-306. <https://doi.org/10.1109/MysuruCon52639.2021.9641731>
- [15] Vojtko, J. (2004). Neural network, component of measuring set for error reduction. *Measurement Science Review*, 4 (1), 1-10.
- [16] Jovanović, J., Denić, D. (2016). A cost-effective method for resolution increase of the two-stage piecewise linear ADC used for sensor linearization. *Measurement Science Review*, 16 (1), 28-34. <https://doi.org/10.1515/msr-2016-0005>
- [17] Kumary, A., Rao, S. (2020). Design techniques of flash ADC: Review. In *Advances in Communication, Signal Processing, VLSI, and Embedded Systems*. Springer, LNEE 614, 89-95. [https://doi.org/10.1007/978-981-15-0626-0\\_8](https://doi.org/10.1007/978-981-15-0626-0_8)
- [18] Waho, T. (2019). Introduction to Analog-to-Digital Converters: Principles and Circuit Implementation (1st ed.). River Publishers, ISBN 9788770221023.
- [19] Thai, H.-H., Pham, C.-K., Le, D.-H. (2023). Design of a low-power and low-area 8-bit flash ADC using a double-tail comparator on 180 nm CMOS process. *Sensors*, 23 (1), 76. <https://doi.org/10.3390/s23010076>
- [20] Chio, U.-F., Wei, H.-G., Zhu, Y., Sin, S.-W., U, S.-P., Martins, R. P., Maloberti, F. (2010). Design and experimental verification of a power effective flash-SAR subranging ADC. *IEEE Transactions on Circuits and Systems II: Express Briefs*, 57 (8), 607-611. <https://doi.org/10.1109/TCSII.2010.2050937>

Received July 12, 2025  
Accepted October 13, 2025